Synthesis and characterization of hybrid fluoro-emulsion based on silica/copolymer composite particles

Ailan Qu,* Xiufang Wen, Pihui Pi, Jiang Cheng and Zhuoru Yang
School of Chemical and Energy Engineering, South China University of Technology, Guangzhou 510640, China

Abstract

BACKGROUND: To create a hydrophobic surface, a commonly used two-step process is the formation of a rough surface and its subsequent modification with materials of low surface energy. Here, a new method for making a hydrophobic surface is proposed using emulsion copolymerization with a low-surface-energy fluoropolymer in the presence of a high percentage of silica particles creating a well-spread roughness.

RESULTS: Irregular core–shell structural composite particles such as of snowman shape and sandwich shape were obtained and characterized. The hydrophobicity and chemical structure of the hybrid film were investigated. It was found that strong inter- and intramolecular chemical bonding in the composite film may improve the properties of the hybrid film. Enrichment of fluorine on the film surface and well-distributed roughness due to the silica particles covered by the fluoropolymer contribute to the increased hydrophobicity of the film. The water contact angle on the film increased from 106 ± 2° to 135 ± 2°.

CONCLUSION: The stable core–shell hybrid latex synthesized in this work will be of use in preparing high-performance hydrophobic aqueous coatings.

Keywords: composite; hybrid fluoro-emulsion; core–shell structure; hydrophobicity

INTRODUCTION

The formation of functional surface films using fluorinated polymers has been a topic of substantial interest owing to their attractive properties such as low surface energy, heat resistance, chemical inertness and low dielectric constant.[1] Hydrophobic coatings may be used in various industrial applications including anti-wetting, anti-snow (or ice) adherence, anti-rusting, reduced friction resistance etc.[2] Among numerous fluorinated polymers, fluorinated acrylic polymers with fluoroalkyl groups have particularly useful characteristics. The pendant $-CF_3$ end groups provide the polymers with extremely low surface energies and the acrylic groups allow the polymers to adhere well to various substrates.[3] Furthermore, organic siloxanes are also used to improve adhesion. They serve as an anchor to the substrate with hydrogen bonds by forming covalent bonds.[4] At the same time, a siloxane may also greatly improve the hydrophobicity of a film surface. The incorporation of an inorganic phase into an organic polymer matrix may be an effective approach to provide improvements in other specific properties of organic polymers.[5] Organic–inorganic hybrids that combine the advantages of both kinds of materials, such as mechanical strength and thermal stability with the processability and flexibility of an organic polymer matrix, exhibit multifunctional characteristics and have been developed as binders for aqueous coatings. Of course, such materials could be obtained by simply mixing the organic and inorganic components. However, in order to achieve a good dispersion of the inorganic compound and to increase interfacial adhesion between the polymer and the mineral, techniques for synthesizing composites made of inorganic particles surrounded by polymers have been developed. Heterogeneous polymerization,[6–20] especially emulsion polymerization,[6–13] provides an effective route and is by far the most frequently used technique. One difficulty of encapsulation reactions through emulsion polymerization resides in the fact that inorganic surfaces are hydrophilic, while polymers are hydrophobic, especially fluorinated acrylates. To our knowledge, to date, there have been few descriptions in the literature of emulsion copolymerizations with reactive emulsifiers, especially with hydrophobic monomers based on fluorinated acrylates, in the presence of a high percentage of SiO_2 particles.

In the work reported here, a composite latex containing a siloxane and a fluorinated copolymer in a shell was prepared by emulsion polymerization in a water medium, using nonionic and reactive anionic

* Correspondence to: Ailan Qu, School of Chemical and Energy Engineering, South China University of Technology, Guangzhou 510640, China
E-mail: elainqal@163.com
(*Received 19 November 2007; revised version received 31 December 2007; accepted 2 June 2008*)
DOI: 10.1002/pi.2477

 Polym Int 0959–8103/2008/$30.00

surfactants as stabilizer, in the presence of silica particles. It has been shown that it would be possible to produce tough hydrophobic nanocomposite coatings by preparing stable organic–inorganic core–shell structural composite nanoparticles with hydrophobic fluorinated acrylate.

EXPERIMENTAL

Materials

The monomer γ-methacryloxypropyltri(isopropoxy) silane (MAPTIPS; $CH_2{=}C(CH_3)COO(CH_2)_3Si(OC_3H_7)_3$) was obtained from Acros Organics Co., USA. The hydrophobic monomer dodecafluoroheptyl methacrylate (DFMA; $CH_2{=}C(CH_3)COOCH_2CF(CF_3)CHFCF(CF_3)_2$) was supplied by XEOGIA Fluorine-Silicon Chemical Co. Ltd, China. The anionic surfactant allyloxy polyoxyethylene(10) nonylammonium sulfate (DNS-86) was obtained from Shuangjian Co. Ltd, Guangzhou, China. Other chemicals were purchased as reagent grade and used without further purification including methyl methacrylate (MMA; 97%), butyl acrylate (BA; 96%), 2-hydroxyethyl methacrylate (HEMA; 98%), sodium hydrogen carbonate ($NaHCO_3$), potassium persulfate (KPS), nonylphenol poly(oxyethylenic) ether (OP-10), tetraethoxysilane (TEOS), ethanol (C_2H_5OH) and ammonia (NH_4OH; 30% in water). Deionized water was used throughout.

Preparation and modification of SiO_2 particles

Silica particles were prepared according to the well-known Stöber method[21] which is very convenient for manipulating the particle size. Ethanol (500 mL) and aqueous ammonia (35 mL) were introduced in a 1000 mL three-neck round-bottom flask equipped with a heat exchange system. The mixture was stirred at 300 rpm to homogenize it and heated to 60 °C. After stabilization, 15 mL of TEOS was added and the mixture was maintained at 60 °C with constant stirring for 24 h to obtain silica of *ca* 80 nm diameter. The modification of the silica beads was carried out by adding MAPTIPS directly into the particle dispersion. The amount of coupling agent was 0.3 g $(g\,SiO_2)^{-1}$. After the mixture was stirred for 12 h at ambient temperature, the reaction medium was heated to 80 °C for 1 h to promote covalent bonding of the organic silane to the surface of the silica nanoparticles.[22] When the synthesis of the silica particles was complete, the main part of the ethanol and ammonia was evaporated under reduced pressure and was replaced with water. The final concentration of silica suspension was determined by measuring the weight.

Preparation of composite latex

The composite emulsion, which contained silica and fluoroacrylic resin in the weight ratio of 0.25:1, was prepared by the emulsion copolymerization of fluoroacrylic monomers in the presence of silica. Following a typical method, a given amount of silica (8 g) suspended in water–ethanol (80 mL at 70:10) and surfactant (0.5 g OP-10/DNS-86 at 50:50 w/w) was transferred into a thermostatted reactor with continuous stirring. A nonionic surfactant (OP-10) and a reactive anionic surfactant (DNS-86) were used as emulsifier at 1.0% (OP-10/DNS-86 = 50:50 w/w) of total solution. After the mixture was stirred for 1 h, the pre-emulsified MMA (15 wt% based on total monomers; the percentages stated below are on the same basis) and initiator KPS solution (1.0 wt% in total) were added dropwise. Then a pre-emulsified mixture of MMA (15%), BA (15%) and HEMA (4%) as a first shell, and a pre-emulsified mixture of BA (13%), DFMA (30%) and MAPTIPS (8%) as a second shell were added sequentially. The total mass of monomers was 200 g L^{-1} and the polymerization started at 75 °C and was complete within 8 h. It was necessary to control the pH value of the initial dispersion (pH = 7.5) using a buffer ($NaHCO_3$) since nanosilica particles show acidic character in the aqueous dispersion.

Silica-free emulsion was also prepared by conventional emulsion copolymerization using the same monomer ratio and different dosages of initiator and emulsifiers as composite emulsion.

Characterization

The sizes and morphologies of composite particles were characterized using transmission electron microscopy (TEM), which can also show the approximate thickness of the shells of core–shell particles. TEM measurements were performed using a Tecnai 10 (Philips Co., The Netherlands) microscope at an accelerator voltage of 200 kV. One drop of the suspension was diluted into water and placed on a carbon-coated copper grid to be dyed with phosphate-tungstic acid for 30 s and dried in air before observation.

The adsorbed or grafted polymer content was determined as follows. The latex was first centrifuged to separate the serum, and then dried under vacuum. Toluene extraction for 8 h under reflux allowed dissolution of the polymer that was simply adsorbed. The residual solid was the silica covered with grafted polymer.[8] The amount of bonded polymer was determined by measuring the difference in weight between the total and the extracted free polymer.

The reaction between the silane coupling agent and nanosilica was evaluated using Fourier transform infrared (FTIR) spectroscopy (VECTOR 33, Bruker Co., Germany) in the 4000–400 cm^{-1} range. The KBr pellet technique was used to prepare powder samples for FTIR studies and the average of three scans for each sample was taken for the peak identification. FTIR analysis was also carried out to determine the chemical structure of the nanosilica/polyacrylate composite latex. TGA/DSC was carried out using a NETZSCH instrument under nitrogen. Initial sample weight was set as 5–8 mg for each operation. The

Polym Int **57**:1287–1294 (2008)
DOI: 10.1002/pi

specimen was heated from −100 to 600 °C at a heating rate of 10 °C min^{-1}.

A film of composite latex was prepared by coating the latex on glass slides to be dried at room temperature for 48 h. X-ray photoelectron spectroscopy (XPS) data were collected in both survey and high-resolution mode using a Krafos Axis Ultra DCD system equipped with an Al Kα source and operating at 150 W. The scanning scope was 700 × 300 μm. Data were recorded at 20°, 40°, 60° and 90° takeoff angles. These angles correspond to an approximate sampling depth of 20–100 Å. Semi-quantification was done by integration of the atomic signals and corrected with sensitivity factors adjusted for the instrument lens and detector design. Atomic force microscopy (AFM) was performed using a Dimension 62 000 nm instrument (CSPM2000). Images were acquired under ambient conditions in tapping mode using a Nanoprobe cantilever. Water contact angle (WCA) was measured with an OCA15 contact angle goniometer from Dataphysics Co., Germany. Typically, the average value of five measurements, made at different positions of the film surface, was adopted as the WCA value. WCA hysteresis (which is equal to the difference between advancing and receding contact angles) was obtained by measuring advancing and receding contact angles after the liquid droplet volume was increased or decreased by 3 μL, respectively.

RESULTS AND DISCUSSION

Microstructure analysis by TEM

Figure 1 shows TEM images of composite latex particles of silica/fluorosiloxane acrylate copolymer, silica/acrylate polymer, pure fluorosiloxane acrylate and silica particles. The pure latex was observed with regular core–shell structure containing fluorine and silicon in the shell (Fig. 1(c)). The light and dark regions in the particles correspond to crosslinked polyacrylate core and fluorinated polyacrylate shell containing siloxane, respectively. The morphology of the latex particles was consistent with the result of a previous paper.[3] The silica particles prepared by the Stöber method shown in Fig. 1(d) demonstrate good particle dispersion. The image of composite particles of modified silica/fluorosilicon acrylate copolymer (Fig. 1(a)) showed a uniform encapsulation, each composite particle containing only one silica seed. But the composite particles are of irregular core–shell structure and of snowman-like or sandwich-like shape with an approximate 20–30 nm shell wrapped on one side of the silica. In comparison with the composite particles of raw silica/acrylate polymer (Fig. 1(b)) free of DFMA and MAPTIPS, the morphology for the modified silica/fluorosilicon acrylate copolymer (Fig. 1(a)) was quite different under the same conditions. It can be concluded for the process of polymerization that MAPTIPS (added together with monomers) has a strong affinity to the silica surface and hydrolyzed rapidly to form silanols which promoted the polymerization of monomer molecules or oligomers directly onto the silica surface. The copolymerization of free molecules of monomers and the methacryloxy groups of MAPTIPS formed oligomers that are expected to be strongly entangled between themselves and around the silica compactly,[8] leading to the formation of a polymer shell. However, the incompatibility between silica and fluoropolymer increased due to the presence of the fluoroacrylate, resulting in the phase separation and leading to the

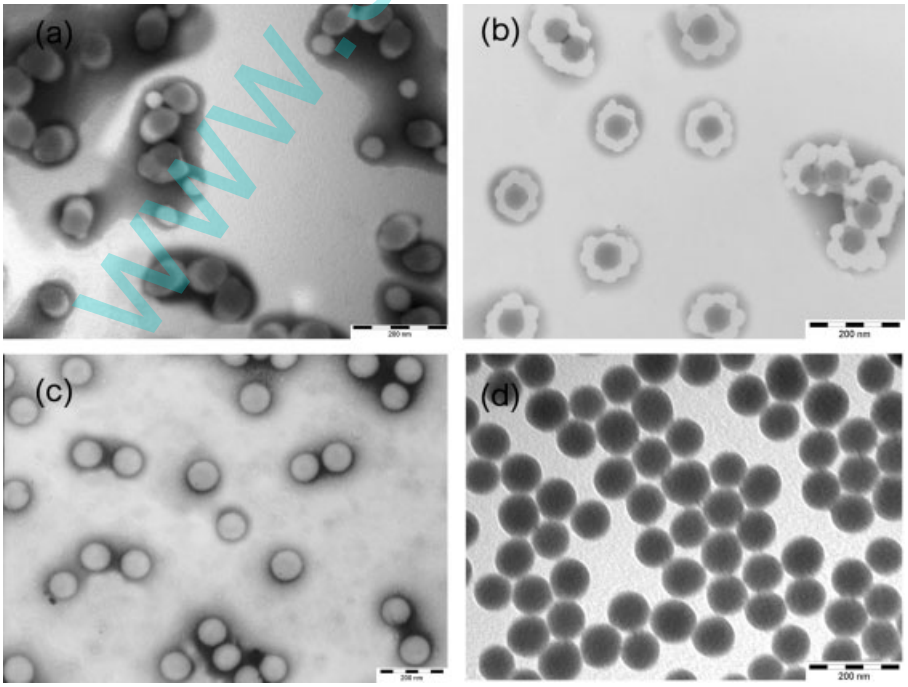

Figure 1. TEM images of composite latex particles: (a) silica/fluorosilicon acrylate copolymer; (b) silica/acrylate polymer; (c) pure fluorosilicon acrylate; (d) silica particles.

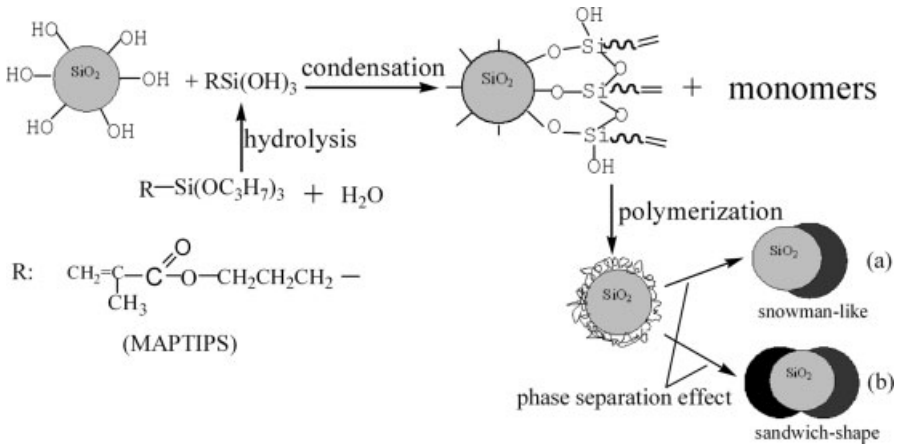

Scheme 1. Schematic of the composite particles formed by emulsion polymerization from modified silica seeds.

formation of irregular core–shell composite particles. The probability of the formation of snowman-like shape is greater than that of sandwich-like shape. The result indicates the obvious phase separation effect though the surface of silica was modified. The process is shown in Scheme 1 and the effects on morphology change are discussed in detail elsewhere.[23]

Qualitative analysis of chemical structure by FTIR

To improve the interfacial adhesion between the silica nanoparticles and polyacrylate molecules, the silane coupling agent was used on the silica.[24] At the interface, the hydroxyl groups of the silane and those on the silica surface can react with each other through Si–O–Si bonding or hydrogen bonding, improving the compatibility and providing reactive groups between the silica and organic monomers. The FTIR spectra of the sol–gel raw silica particles and modified silica particles are shown in Fig. 2. A broad band at 3440 cm^{-1} demonstrates the presence of hydroxyl groups on the surface. The absorption band between 800 and 1260 cm^{-1} has been described as a superimposition of various SiO_2 peaks,[25] including the specific adsorption bands of silica at 1100 cm^{-1} for the asymmetric stretch vibration of Si–O–Si, 800 cm^{-1} for Si–O–Si bending, 467 cm^{-1} for Si–O–Si swing and 970 cm^{-1} for Si–OH stretching. An absorption corresponding to the H–O–H bending vibration at 1633 cm^{-1} is also seen, indicating residual intramolecular water inside the silica nanoparticles.[26] The presence of residual hydroxyl groups on the surface of modified silica showed that not all of the hydroxyl groups on the surface of silica particles reacted with siloxane molecules. Also, bands appeared at 1710 cm^{-1} for the C=O group, showing successful grafting of the siloxane molecules onto the surface of silica particles.

The FTIR spectra of fluorosiloxane acrylate emulsion and composite latex are shown in Figs 2(a) and (d), respectively. In both spectra, it can be seen that a strong adsorption peak appeared at 2963 cm^{-1} for

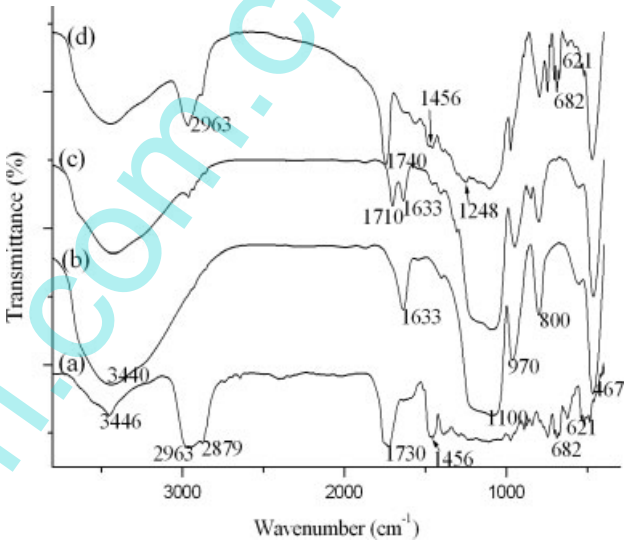

Figure 2. FTIR spectra of (a) pure emulsion film, (b) raw silica particles and (c) modified silica and (d) hybrid film.

$-CH_2$ groups and a broad band around 3446 cm^{-1} for –OH groups. The peak at about 1456–1400 cm^{-1} in the FTIR spectra of pure film and composite films is the characteristic absorption of carboxyl and methylene groups in monomers and signals at 1248, 682 and 621 cm^{-1} are assigned to C–F stretching and wagging vibrations. In the composite latex, the absorption bands corresponding to the C–OH and C–O–C groups of the polyacrylate chains were mostly overlapped by strong absorption in the region ranging from 1000 to 1300 cm^{-1} because of the stretching vibration of Si–O–Si in the hybrids. Also the peaks at 1145 cm^{-1} corresponding to characteristic absorption of CF_3 groups could not be clearly distinguished.[27] However, the FTIR spectrum of composite latex had all the characteristic bands of nanosilica and pure polyacrylate latex and did not indicate a simple combination of both the FTIR spectra; for example, the absorption of the carbonyl bonding is slightly different between the pure polyacrylate latex and composite latex. The peak of the C=O stretching vibration shifts from 1730 cm^{-1} in the pure polyacrylate latex

to 1740 cm^{-1} in the composite latex because of the effect of the intramolecular hydrogen bonding between the nanosilica and polyacrylate chains. The increased intensity of the Si–O–Si band indicated the successful incorporation of silica in the hybrid films. For the sample of raw silica/acrylate composite particles, 61 wt% of the total amount of polymer surrounding the silica beads was adsorbed, whereas 39 wt% was grafted. For modified silica/fluorosiloxane acrylate composite particles, the result showed that 86 wt% of the total polymer surrounding the beads was grafted, whereas 14 wt% was dissolved. From the difference in the FTIR spectra between the fluorosiloxane acrylate latex and the composite latex and the measured graft ratio, it could be concluded that strong intermolecular chemical bonding tethered the nanosilica and polyacrylate chains in the composite film.[28]

Quantitative analysis of surface composition by XPS

To confirm the existence of fluorine-containing groups on the layer of the prepared film, XPS spectra of pure and hybrid film were obtained. Comparing the binding energy and spectra between the two, both of them are similar with respect to F_{1s}, O_{1s} and C_{1s}. The F_{1s} window shows a singular symmetrical peak at 689.1 ± 0.1 eV, and the O_{1s} window shows two peaks with similar areas at 533.8 ± 0.1 and 532.3 ± 0.1 eV, respectively, corresponding to the two different types of oxygen in the ester functional group. The C_{1s} window shows a complex pattern of peaks which represents four kinds of carbon bonds (289.3 eV possibly due to C–F or C=O, the peak overlap resulting from the binding energy of any CF groups (*ca* 289.6 eV) to be indistinguishable from that of C=O (289.4 eV); CF_3 at 293.8 eV; C–O at 286.1 eV; and C–C at 285.0 eV). The C–Si peak at 284.2 eV is too small to be discerned. These results show the similar chemical environment of F, C and O atoms in both cases, apart from the chemical shift of the Si_{2p} binding energy for Si–O group from 102.1 eV in pure film to 103.1 eV induced by the silica in hybrid film. Typical survey and C_{1s} spectra for the film surface are shown in Fig. 3.

The elements on different layers of the film surface are given in Table 1. Analysis performed at various takeoff angles of 20°, 40°, 60° and 90° may provide a means to probe both the surface and deep features of this material. The quantitative evaluation of the XPS spectra was carried out by determining the areas of

Table 1. XPS data for the film surfaces

	Pure latex (at.%)				Hybrid latex (at.%)			
Takeoff angle (°)	F	C	O	Si	F	C	O	Si
20	28.8	59.1	10.5	1.6	29.1	48.0	20.2	2.7
40	27.4	58.4	13.1	1.1	28.9	48.3	20.1	2.6
60	26.3	58.1	14.2	1.4	28.7	48.3	20.4	2.6
90	21.5	64.4	12.5	1.5	23.6	57.0	17.3	2.1

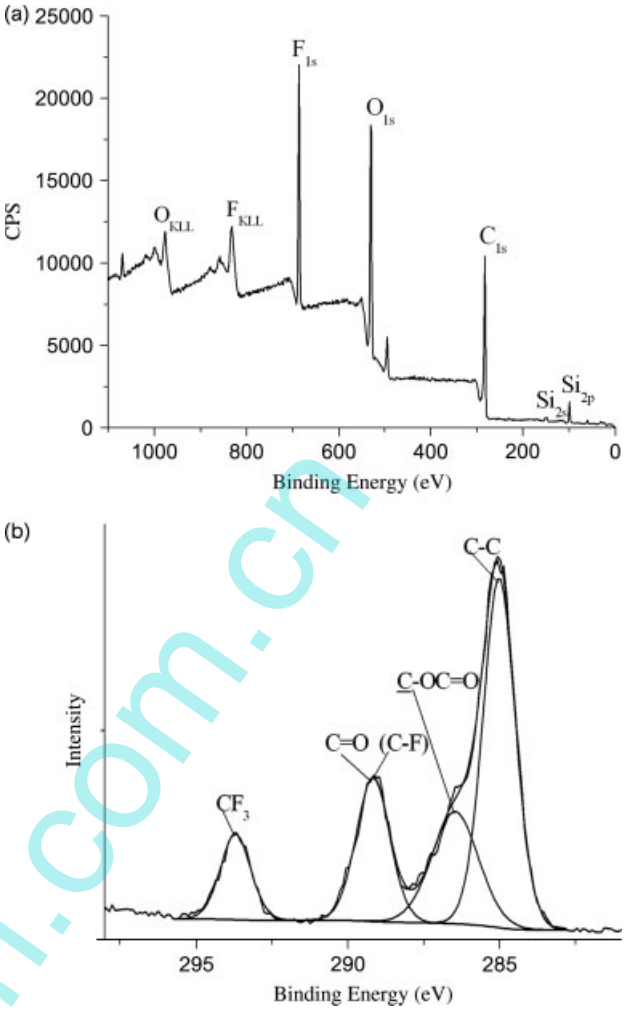

Figure 3. XPS spectra of hybrid film: (a) survey; (b) C_{1s} spectrum.

the C_{1s}, F_{1s}, O_{1s} and Si_{2p} peaks and multiplying them to obtain the appropriate sensitivity factors. As can be seen from Table 1, in both cases, the fluorine content on the surface is higher than that in the bulk (fluorine theoretical content is 20.35%, assuming 100% conversion of emulsion polymerization) and it decreases with depth into the film. This indicates, as anticipated, that the fluorocarbon side chain enriches preferentially on the surface compared to the acrylate backbone and a gradient of fluorine occurs from the surface into the bulk of the polymer film. On the other hand, there is an increase of fluorine content in each layer indicating that the modified silica particles improve the migration and enrichment of fluorine-containing chain segments towards the surface. This probably results from phase separation between silica and fluorocopolymer. The silicon distribution of the hybrid film, however, was very different from that of the pure emulsion film. For the pure film, the silicon content shows bidirectional variations in concentration, probably because the MAPTIPS exhibits a similar propensity as fluorine for the surface and may also serve as an anchor to the substrate by forming covalent bonds. For the hybrid film, however, it decreased with etching depth and was slightly higher than that of the pure film in each layer. This may

be interpreted by the addition of silica modified with silane coupling agent resulting in the increase of silicon in the bulk of the hybrid film.

Thermal analysis

The thermal decomposition behavior of the pure polyacrylate film and hybrid films was investigated by TGA at a heating rate of 10 °C min^{-1} under a nitrogen flow, as illustrated in Fig. 4(a), which shows the TGA curves of fluorosiloxane acrylate, raw silica/acrylate and modified silica/fluorosiloxane acrylate. The order of the thermal decomposition temperature is (1) fluorosiloxane acrylate, (2) raw silica/acrylate and (3) modified silica/fluorosiloxane acrylate. This suggests the enhancement of the degree of crosslinking and thermal stability was brought about by the incorporation of siloxane and modified silica. At the same time, it is also evident that the temperature of glass transformation increased in Figs 4(b) and (d) compared with Fig. 4(c) because the presence of fluoromonomer and siloxane leads to a high degree of crosslinking. The increasing residue for samples (2) and (3) at 420 °C suggested the successful incorporation of the silica in the hybrid materials. All the polymer components will essentially have decomposed before reaching 600 °C in nitrogen atmosphere, and the remaining residue reflects the silicone oxide content. The residue of raw silica/polyacrylate is 23.2 wt%, approximately comparable to the TGA residue, while the amount of modified silica/fluorosiloxane acrylate is higher than 32 wt%. The higher experimental residue for sample (3) is probably due to the trapping of highly crosslinked polymer resulting from the condensation between silanol generated by the hydrolysis of MAPTIPS and hydroxyls on the surface of the silica, although hydrogen bonds occur between the C=O of organic polymer and the silanols of the inorganic networks. Usually, the hydrogen bond is much less effective than the condensation between the $-Si(OH)_3$ groups generated by the hydrolysis and the hydroxyls of silica. The weight loss of raw silica/acrylates is higher than that of fluorosiloxane acrylate and that of silica/fluorosiloxane acrylate at temperatures lower than 300 °C and an exothermic reaction was retained for temperatures of 100–300 °C as shown by the DSC curve in Fig. 4(c). It can be elucidated that some low-molecular-weight polymers that decomposed earlier brought about retardation of the polymerization due to the presence of raw silica.

Surface topographic analysis by AFM

AFM was employed to observe the surface morphologies of different films (Fig. 5). The parameters of root-mean-square (S_q, giving the standard deviation of the height values), roughness average (R_a) and roughness factor ($R = 1 + S_{dr}$, where S_{dr} is surface area ratio between the interfacial and projected areas)[29] were obtained from AFM software analyses over a scope of 50 × 50 μm. Values of R_a and S_q for pure fluorinated film are found to be 0.8 and 1.1, respectively. The pure film is smooth, with a value of R of nearly 1.00,

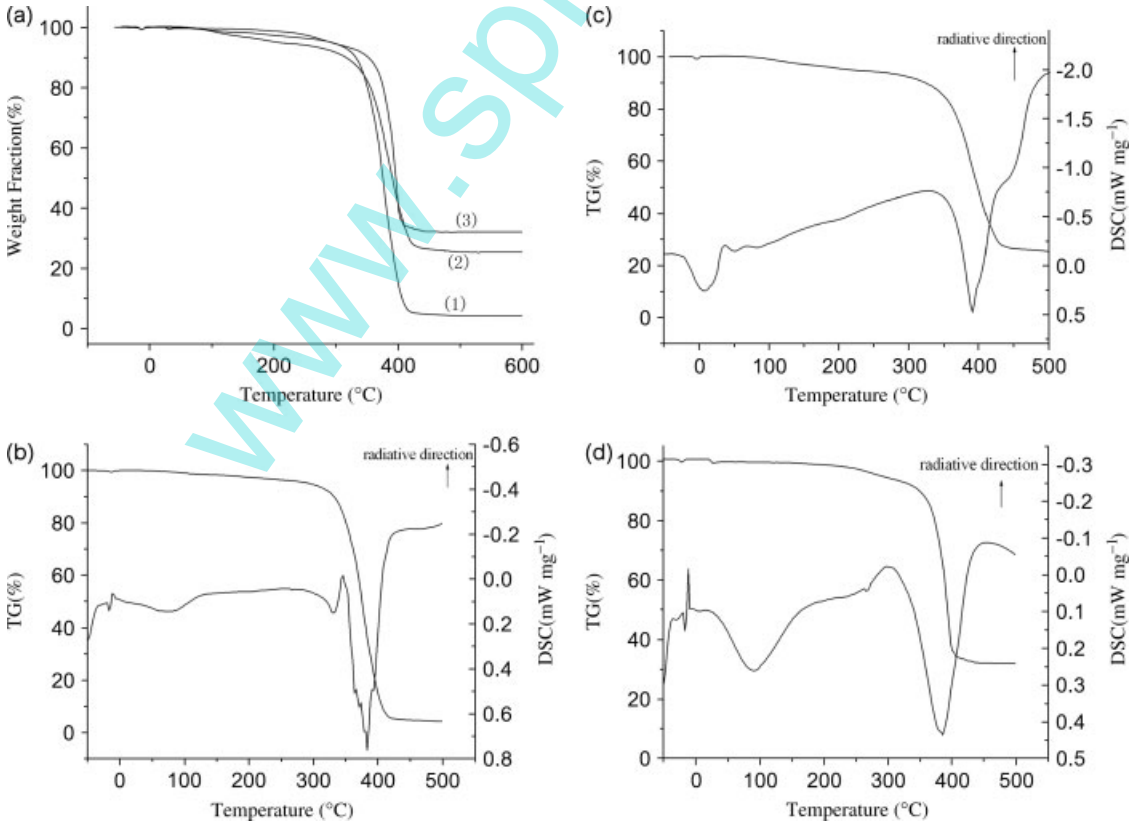

Figure 4. TGA/DSC curves. (a) TGA curves of fluorosiloxane acrylate (1), raw silica/acrylate (2) and modified silica/fluorosiloxane acrylate (3). TGA/DSC curves of (b) (1); (c) (2); (d) (3).

Polym Int **57**:1287–1294 (2008)
DOI: 10.1002/pi

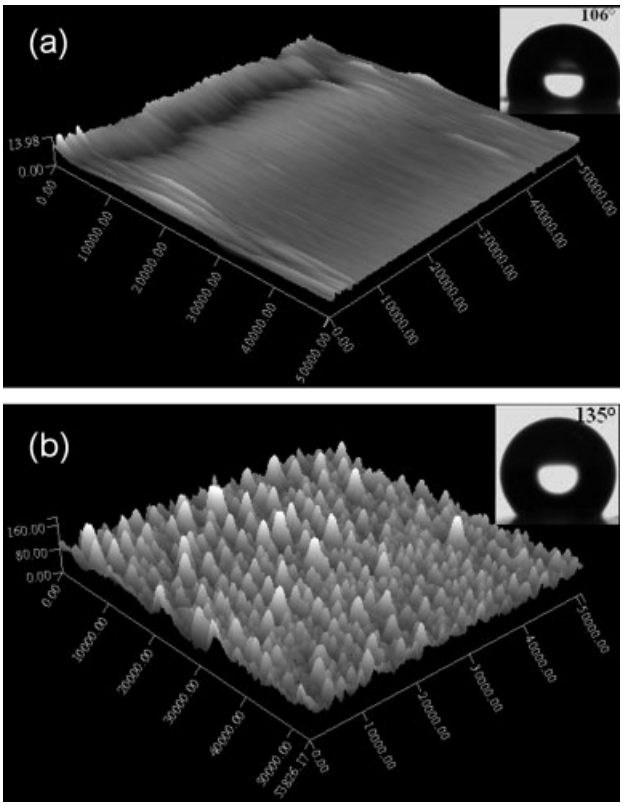

Figure 5. AFM images of (a) pure film and (b) hybrid film. The insets show the water contact angles.

which can be seen in the AFM image of Fig. 5(a). For the nanocomposite film, the R value is 1.44, and R_a and S_q are 21.0 nm and 29.0 nm, respectively. On the surface of the hybrid film, there is a small number of summits (Fig. 5(b)) and the roughness factors increased, indicating that silica particles move to the surface and increase the micro-roughness on the surface during the process of film formation. On the other hand, the condensation between the silanol functional groups on the SiO_2 surface and the hydrolyzed MAPTIPS facilitated the enrichment of SiO_2 particles on the film surface.

Hydrophobicity of film surface

The contact angles of water on different films tested were consistent with the topographic analysis discussed above. The contact angle on the pure fluorinated film is $106 \pm 2°$, while that on the hybrid film is $135 \pm 2°$. The WCA hysteresis for pure and hybrid films was $12 \pm 1°$ and $20 \pm 1°$. It is well known that the WCA is not only governed by the surface energy of the materials but also by the surface roughness and structure. The surface roughness can change the contact angles as chemicals do but through a different mechanism. Two distinct models have been proposed to explain this phenomenon: the Wenzel model and the Cassie model.[30] The Wenzel model describes a roughness regime in which both advancing WCA and WCA hysteresis increase as r increases (water penetrates into the surface cavity). The apparent water contact angle calculated from the Wenzel model (113°, based on the 106° WCA of a flat fluorinated surface) is lower than the experimental value (135°) obtained in this work. For a composite surface, the WCA is described by the Cassie–Baxter equation as follows: $\cos\theta_r^c = f \cos\theta + f - 1$, where f is the area fraction of the solid in contact with the liquid. From the Cassie model, the value of f was calculated to be 0.404 which may indicate that the water drop may not penetrate thoroughly the surface grooves on the films. This result is consistent with the XPS analysis which also indicated that modified silica particles improved the migration and enrichment of fluorine-containing chain segments towards the surface.

CONCLUSIONS

By introducing modified silica nanoparticles into the polymerization of fluorinated acrylate–siloxane monomers, an organic–inorganic composite latex with irregular core–shell structure was obtained. Strong chemical bonding was found to link the nanosilica and polymer chains and form the core–shell structural composite latex, improving the properties of the latex. The roughness of the film surface and enrichment of fluorine on it increased due to the irregular core–shell structure of silica seeds covered with fluoropolymer. The results of contact angle measurement support the AFM and XPS analyses. The method is suggested as a way to improve the properties of hydrophobic coatings by preparing organic–inorganic composite latex with a core–shell structure.

REFERENCES

1 Jeyaprakash JD, Samuel S and Rühe J, *Langmuir* **20**:10080 (2004).
2 Yoshida N, Abe Y, Shigeta H, Takami K, Osaki H, Watanabe T, *et al*, *J Sol-Gel Sci Technol* **31**:195 (2004).
3 Cui X, Zhong S and Wang H, *Polymer* **48**:7241 (2007).
4 Genzer J and Efimenko K, *Science* **290**:2130 (2000).
5 Bauer F, Gläsel HJ, Decker U, Ernst H, Freyer A, Hartmann E, *et al*, *Prog Org Coat* **47**:147 (2003).
6 Luna-Xavier JL, Guyot A and Bourgeat-Lami E, *J Colloid Interface Sci* **250**:82 (2002).
7 Luna-Xavier JL, Bourgeat-Lami E and Guyot A, *Colloid Polym Sci* **279**:947 (2001).
8 Espiard Ph and Guyot A, *Polymer* **36**:4391 (1995).
9 Corcos F, Bourgeat-Lami E and Lang J, *J Colloid Interface Sci* **210**:281 (1999).
10 Perro A, Reculusa S, Bourgeat-Lami E, Duguet E and Ravaine S, *Colloids Surf A: Physicochem. Eng. Aspects* **284–285**:78 (2006).
11 Reculusa S, Poncet-Legrand C, Perro A, Duguet E, Bourgeat-Lami E, Mingotaud C, *et al*, *Chem Mater* **17**:3338 (2005).
12 Reculusa S, Mingotaud C, Bourgeat-Lami E, Duguet E and Ravaine S, *Nano Lett* **4**:1677 (2004).
13 Reculusa S, Poncet-Legrand C, Ravaine S, Mingotaud C, Duguet E and Bourgeat-Lami E, *Chem Mater* **14**:2354 (2002).
14 Zhang SW, Zhou SX, Weng YM and Wu LM, *Langmuir* **21**:2124 (2005).
15 Percy MJ, Michailidou V and Armes SP, *Langmuir* **19**:2072 (2003).

16 Tong X, Tang T, Zhang Q, Feng ZL and Huang BT, *J Appl Polym Sci* **83**:446 (2002).
17 Antonietti M and Landfester K, *Prog Polym Sci* **27**:689 (2002).
18 Sondi I, Fedynyshyn TH, Sinta R and Matijevic E, *Langmuir* **16**:9031 (2000).
19 Barthet C, Hickey AJ, Cairns DB and Armes SP, *Adv Mater* **11**:408 (1999).
20 Corcos F, Bourgeat-Lami E, Novat C and Lang J, *J Colloid Polym Sci* **277**:1142 (1999).
21 Stöber W, Fink A and Bohn E, *J Colloid Interface Sci* **26**:62 (1968).
22 Westcott SL, Oldenburg SJ, Randall LT and Halas NJ, *Langmuir* **14**:5396 (1998).
23 Qu A, Wen X, Pi P, Cheng J and Yang Z, *J Colloid Interface Sci* **317**:62 (2008).
24 Yang R, Liu Y, Wang K and Yu J, *J Anal Appl Pyrolysis* **70**:413 (2003).
25 Yu YY and Chen WC, *Mater Chem Phys* **82**:388 (2003).
26 Wang Y, Li Y, Zhang R, Huang L and He W, *Polym Compos* **27**:282 (2006).
27 Yu ZG, Zhang ZB, Yuan QL and Ying SK, *Adv Polym Technol* **21**:268 (2002).
28 Huang SL, Chin WK and Yang WP, *Polymer* **46**:1865 (2005).
29 Peltonen J, Järn M, Areva S, Linden M and Rosenholm JB, *Langmuir* **20**:9428 (2004).
30 Erbil HY, Demirel AL, Avci Y and Mert O, *Science* **299**:1377 (2003).

Polym Int **57**:1287–1294 (2008)
DOI: 10.1002/pi